Received: 25 May 2024 | Revised: 29 September 2024 | Accepted: 15 October 2024

DOI: 10.1111/mpp.70021

Molecular Plant Pathology WILEY

ORIGINAL ARTICLE

The *Phytophthora infestans* effector Pi05910 suppresses and destabilizes host glycolate oxidase StGOX4 to promote plant susceptibility

Peiling Zhang[1] | Jinyang Li[2] | Xiuhong Gou[2] | Lin Zhu[1] | Yang Yang[1,2] | Yilin Li[1] | Yingqi Zhang[1] | Liwen Ding[1] | Assiya Ansabayeva[3] | Yuling Meng[1] | Weixing Shan[1]

[1]State Key Laboratory of Crop Stress Biology for Arid Areas and College of Agronomy, Northwest A&F University, Yangling, Shaanxi, China

[2]State Key Laboratory of Crop Stress Biology for Arid Areas and College of Plant Protection, Northwest A&F University, Yangling, Shaanxi, China

[3]Department of Agronomy, A. Baitursynov Kostanay Regional University, Kostanay, Kazakhstan

Correspondence
Weixing Shan, State Key Laboratory of Crop Stress Biology for Arid Areas and College of Agronomy, Northwest A&F University, Yangling, Shaanxi 712100, China.
Email: wxshan@nwafu.edu.cn

Funding information
Key Research and Development Projects of Shaanxi Province, Grant/Award Number: 2021LLRH-07; Program of Introducing Talents of Innovative Discipline to Universities from the State of Administration for Foreign Experts Affairs, China, Grant/Award Number: B18042; China Agriculture Research System, Grant/Award Number: CARS-09

Abstract

Phytophthora infestans is a notorious oomycete pathogen that causes potato late blight. It secretes numerous effector proteins to manipulate host immunity. Understanding mechanisms underlying their host cell manipulation is crucial for developing disease resistance strategies. Here, we report that the conserved RXLR effector Pi05910 of *P. infestans* is a genotype-specific avirulence elicitor on potato variety Longshu 12 and contributes virulence by suppressing and destabilizing host glycolate oxidase StGOX4. By performing co-immunoprecipitation, yeast-two-hybrid assays, luciferase complementation imaging, bimolecular fluorescence complementation and isothermal titration calorimetry assays, we identified and confirmed potato StGOX4 as a target of Pi05910. Further analysis revealed that *StGOX4* and its homologue *NbGOX4* are positive immune regulators against *P. infestans*, as indicated by infection assays on potato and *Nicotiana benthamiana* overexpressing *StGOX4* and TRV-*NbGOX4* plants. *StGOX4*-mediated disease resistance involves enhanced reactive oxygen species accumulation and activated the salicylic acid signalling pathway. Pi05910 binding inhibited enzymatic activity and destabilized StGOX4. Furthermore, mutagenesis analyses indicated that the 25th residue (tyrosine, Y25) of StGOX4 mediates Pi05910 binding and is required for its immune function. Our results revealed that the core RXLR effector of *P. infestans* Pi05910 suppresses plant immunity by targeting StGOX4, which results in decreased enzymatic activity and protein accumulation, leading to enhanced plant susceptibility.

KEYWORDS
glycolate oxidase, *Phytophthora infestans*, plant immunity, reactive oxygen species, RXLR effector

1 | INTRODUCTION

Potato (*Solanum tuberosum*) has become an essential food crop worldwide. Potato production is seriously threatened by various microbial pathogens, including the most notorious *Phytophthora infestans* that caused the Irish Great Famine. Plants usually activate defence responses when they sense signals from microbes. Pathogen/microbe-associated molecular patterns (P/MAMPs) recognized by plasma membrane-localized pattern recognition receptors (PRRs)-triggered immunity (PTI) are the first layer of plant defence against pathogens (Jones & Dangl, 2006). The complex signal pathway network in PTI is inseparable from the identification of PAMPs (Garcia & Steinbrenner, 2023). The PRR protein FLS2 recognizes flg22, a conserved small peptide from bacterial flagellin, as a PAMP molecule that can inhibit the burst of reactive oxygen species (ROS), callose deposition and expression of defence genes (Cabre et al., 2024; Dewangan et al., 2023). A further proactive defence of plants is to activate faster and stronger effector-triggered immunity (ETI) by plant nucleotide-binding leucine-rich repeat proteins (NLRs) directly or indirectly recognizing effector proteins secreted by pathogens (Jones & Dangl, 2006). ETI causes a hypersensitive response (HR) in cells, thus restricting pathogens to specific regions (Jones & Dangl, 2006). One of the best-studied *P. infestans* RXLR effectors is PiAvr3a, which confers avirulence in *R3a*-containing potatoes; the *R3a* and *PiAvr3a*-mediated incompatibility interaction has recently been well studied also at the transcriptome level (Xue et al., 2021).

When not recognized by the NLRs, RXLR effector proteins facilitate pathogen colonization by modulating plant immunity in different plant subcellular compartments (Braet et al., 2022; Chen et al., 2020; Wang et al., 2019). For instance, the RXLR effector PsCAP1 from *Phytophthora sojae* requires plasma membrane localization of LRR-RLP and LRR-RLKs to trigger plant immunity (Jiang et al., 2023). *Phytophthora capsici* RXLR effector PcAvr3a12 inhibits PPIase to suppress endoplasmic reticulum (ER)-mediated immunity (Fan et al., 2018). *P. infestans* RXLR effectors AVR1 and PexRD31 suppress plant immunity by associating with components of vesicle trafficking machinery (Du et al., 2015; Petre et al., 2021).

ROS are important signalling molecules in plant immunity and regulate cellular mechanisms under abiotic and biotic stresses in different subcellular compartments (Giulietti et al., 2023). H_2O_2 is one of the main forms of ROS, and its mechanism of interaction or signalling pathway with plants has become a focus in plant immunity studies in recent years. For example, *Plasmopara viticola* effector RXLR50253 targets VpBPA1 and attenuates plant immunity by reducing the accumulation of H_2O_2 during pathogen infection (Yin et al., 2022). *P. viticola* effector RXLR31154 and its target VpPsbP reduce H_2O_2 accumulation and activate the $^1O_2$ signalling pathway (Liu et al., 2021). About 70% of H_2O_2 in C3 plants comes from the substrate oxidation process of glycolate oxidase in photorespiration (Foyer et al., 2009; Noctor et al., 2002). Glycolate oxidase (GOX), a member of the FMN (flavin mononucleotide)-dependent α-hydroxy acid oxidase family, is encoded by nuclear genes, synthesized on cytoplasmic ribosomes and transported to peroxisomes (Olsen & Harada, 1995). GOX converts glycolate into glyoxylate and produces H_2O_2 in the photorespiration pathway (Liu et al., 2018). The hydroxy acid oxidase (*HAOX*) gene family, a subfamily of the GOX family, has similar activity (Mariyam et al., 2023). *Arabidopsis thaliana* encodes three paralogous GOX proteins (AtGOX1-3) and two HAOX proteins (AtHAOX1-2) (Reumann et al., 2004), while *Nicotiana benthamiana* encodes seven (NbGOX1-7) and nine proteins (NbHAOX1-10), respectively (Xu et al., 2018).

GOX has been reported to be involved in biotic and abiotic stresses in plants. For example, melatonin supplementation significantly reduced the enzymatic activity of GOX in drought-stressed tomato plants (Khan et al., 2024). Arsenate treatment enhanced the GOX activity in *Vicia faba*, whereas simultaneous treatment with melatonin and Ca^{2+} noticeably reduced it under arsenate stress (Siddiqui et al., 2020). The role of AtGOX1 and AtGOX3 in resistance against the non-host pathogen *Pseudomonas syringae* pv. *tabaci* does not depend on NADPH oxidase (Rojas & Mysore, 2012). Members of NbGOX family are involved in distinct defence pathways to affect resistance of *N. benthamiana* to tobacco rattle virus (TRV), *Xanthomonas oryzae* pv. *oryzae* and *Sclerotinia sclerotiorum*. NbGOX4 might function through suppressing NbHAOX8 and NbGOX1 (Xu et al., 2018). *A. thaliana* plants overexpressing *GOX* show improved resistance mediated by *WRKY33* against *Colletotrichum higginsianum* (Schmidt et al., 2020). The GOX activity of *A. thaliana* leaves increased in an effector DspA/E-dependent manner by *Erwinia amylovora*, a non-host pathogen, and *gox2-2* mutants were more sensitive to infection by this pathogen (Launay et al., 2022).

Phytohormones such as salicylic acid (SA) play crucial roles in plant immune responses (Ding & Ding, 2020; Zhang & Li, 2019), inducing expression of defence genes such as *PATHOGENESIS RELATED* (*PR*), and ultimately establish systemic acquired resistance (SAR) (Han et al., 2022b; Han, Tan, et al., 2022). *A. thaliana ETHYLENE RESPONSIVE FACTOR 19* (*ERF019*) knockout mutant (*erf019*) shows enhanced resistance to *P. parasitica* and upregulated expression of *PR1* (Lu et al., 2020). ROS and SA signalling pathways are both involved in the activation of plant defence responses. PvAvh77-M2, a truncated form of PvAvh77, activates the SA and H_2O_2 signalling pathways to enhance resistance to *P. viticola* (Fu et al., 2023). Exogenous SA stimulation can affect the physical binding and dissociation of GOX and catalase (CAT), thereby regulating endogenous H_2O_2 levels (Li et al., 2021; Zhang et al., 2016).

In this work, we focus on *P. infestans* effector Pi05910-mediated immune suppression and molecular dissection of its target StGOX4-mediated immunity. We show that Pi05910 has genotype-specific elicitor function in potato cultivar Longshu 12. We demonstrate that Pi05910 has virulence function, targeting the host protein StGOX4, which acts as a positive immune regulator. Pi05910 binding to StGOX4 interferes with ROS and SA signalling pathways and inhibits the enzymatic activity and stability of StGOX4. This research highlights a mechanism by which *P. infestans* promotes infection by interfering with *GOX4*-mediated host defence responses.

2 | RESULTS

2.1 | Pi05910 is an avirulence elicitor with virulence contribution and its nuclear localization is required for virulence function

The RXLR effector Pi05910 is highly conserved in *P. infestans* isolates from China and its expression is highly upregulated in the early stages of infection, suggesting its importance as a candidate core effector (Yin et al., 2017). Agroinfiltration-mediated transient expression of *35S::Pi05910-GFP* construct, encoding the C-terminus GFP-tagged Pi05910, showed it has potato genotype-specific elicitor function in Longshu 12 (Figure S1a). Infiltration assays in potato leaves with purified recombinant His-Pi05910 protein from *Escherichia coli* confirmed Pi05910 has avirulence function in Longshu 12, which also suggests it is a biologically active form of the recombinant effector protein Pi05910 (Figure S1b). Therefore, we further tested the virulence function by transient expression of *35S::Pi05910-GFP* in *N. benthamiana* leaves followed by inoculation with *P. infestans* zoospores. Pi05910-GFP significantly increased susceptibility of *N. benthamiana* to *P. infestans*, as indicated by larger lesion diameters (Figure 1b, Figure S2a). These results indicated that Pi05910 has both elicitor and virulence function.

To examine subcellular localization of Pi05910, we transiently expressed *35S::Pi05910-GFP* fusion construct in *N. benthamiana* by agroinfiltration. Confocal microscopy observation showed that it overlapped with the nuclear fluorescent dye 4′,6-diamidino-2-phenylindole (DAPI) (Linhoff et al., 2015) and the cytoplasmic marker UGP1-mCherry (Furtauer et al., 2019) (Figure 1a), indicating that Pi05910 is localized in both the nucleus and cytoplasm. In order to explore which subcellular localization is responsible for the virulence of Pi05910, we fused a nuclear export signal (NES) to the C-terminus of Pi05910, *35S::Pi05910-GFP*$_{NES}$. Transient expression and confocal microscopy assays showed that Pi05910-GFP$_{NES}$ was no longer localized in the nucleus (Figure 1a). Inoculation with *P. infestans* showed that Pi05910-GFP$_{NES}$ lost its virulence, as indicated by the similar lesion sizes with the FLAG-GFP control (Figure 1b). Western blotting analysis confirmed protein expression and integrity (Figure S2b,c). Furthermore, Pi05910-GFP$_{NES}$ lost the ability to trigger cell death on Longshu 12 (Figure S1c). These results indicate that nuclear localization is required for the virulence and elicitor functions of Pi05910.

2.2 | Pi05910 targets glycolate oxidase NbGOX4 and its potato orthologue StGOX4

To obtain insight into the mechanisms of Pi05910-mediated suppression of plant immunity, we transiently expressed *35S::Pi05910-GFP* (without the signal peptide) in *N. benthamiana* and performed immunoprecipitation assays with anti-GFP trap followed by liquid chromatography-mass spectrometry/mass spectrometry (LC–MS/MS). Yeast two-hybrid (Y2H) assays of 10 candidate target proteins (Table S1) determined that NbGOX4 (Niben101Scf04174g05001.1) interacted with Pi05910 (Figure 2a). Protein sequence alignments of NbGOX4 in the *S. tuberosum* database (https://solgenomics.net/tools/blast/) led to the identification of StGOX4 (PGSC0003DMT400071115), with over 95% sequence similarity (Figure S3a), which was also shown to interact with Pi05910 (Figure 2a). StGOX4 shares the closest phylogenetic relationship with NbGOX4 (Figure S3b). We further confirmed the interaction between Pi05910 and NbGOX4 or StGOX4 by luciferase complementation imaging (LCI) in vivo and co-immunoprecipitation (Co-IP) assays (Figure 2b,c). The results were consistent with that of Y2H assays. We expressed recombinant protein in *Escherichia coli* followed by affinity purification of Pi05910 and NbGOX4 and StGOX4 (Figure S4a,b). Isothermal titration calorimetry (ITC) assays showed the binding affinity of His-Pi05910 with His-NbGOX4 and His-StGOX4 was 1.233 and 4.022 μM, respectively (Figure 2d). To determine the subcellular localization of the Pi05910 and StGOX4 interaction, we performed bimolecular fluorescence complementation (BiFC) assays. The results showed that cYFP-Pi05910 interacts with nYFP-StGOX4 in the host nucleus and cytoplasm (Figure 2e). Thus, these assays confirmed that the effector protein Pi05910 interacts with NbGOX4 and StGOX4.

To examine subcellular localization of StGOX4, we expressed a construct of StGOX4 fused with GFP (*35S::GFP-StGOX4*) in *N. benthamiana* with an mCherry-fused peroxisome marker PTS2 (*35S::mCherry-PTS2*) (Kunze, 2020) as a standard control. Confocal microscopy observation indicated that StGOX4 accumulated in the cytoplasm, nucleus and peroxisomes (Figure S5a). Total protein and nuclear protein extraction indicated the expression and integrity of fusion proteins (Figure S5a). To determine co-localization of Pi05910 with StGOX4, *35S::Myc-mCherry-StGOX4* and *35S::Pi05910-GFP* were co-expressed by agroinfiltration, and confocal microscopy showed their co-localization in the cytoplasm and nucleus (Figure S5b).

2.3 | StGOX4 positively regulates plant immunity against *P. infestans*

To explore the expression profile of *StGOX4* during *P. infestans* infection, we collected leaf samples of *P. infestans*-infected Longshu 12 at different time points for reverse transcription-quantitative PCR (RT-qPCR) analysis. The results showed that the expression of *StGOX4* was downregulated during *P. infestans* infection (Figure S6). To explore the immune function of *StGOX4*, we generated stable overexpression (OE) transformants of potato cv. Atlantic. Three independent lines, OE21, OE29 and OE38 with increased *StGOX4* transcript levels, as confirmed by RT-qPCR, were selected for further analysis (Figure S7a). The phenotypes of transgenic plants were not significantly different to the wild-type Atlantic (Figure S7b). *P. infestans* infection assays showed reduced lesion expansion and limited *P. infestans* colonization in OE-*StGOX4* lines (Figure 3a). We also constructed an RNAi-*StGOX4* vector and performed stable transformation of potato. However, the stem segment could not form callus

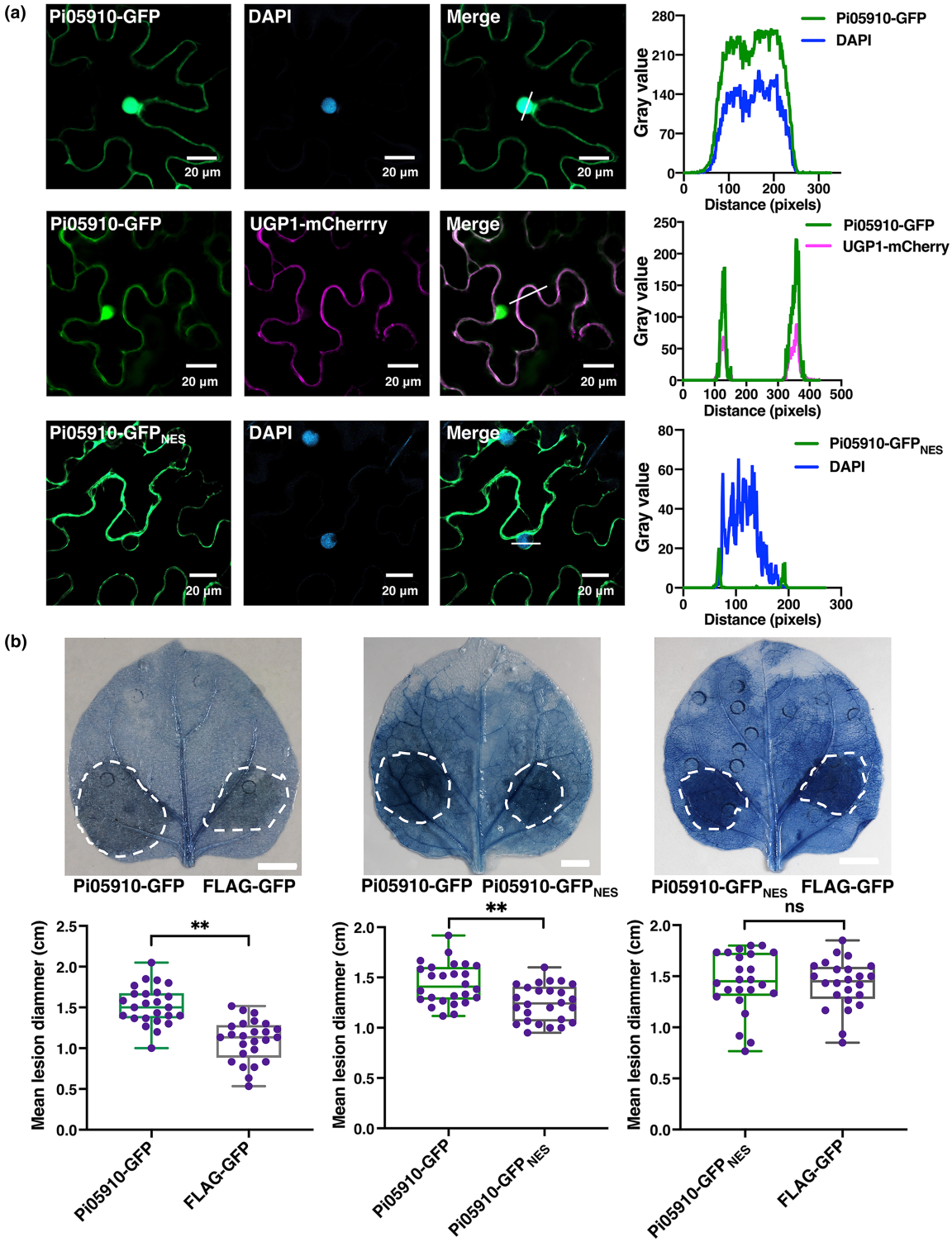

FIGURE 1 Nuclear localization of *Phytophthora infestans* effector Pi05910 is required for promoting plant susceptibility. (a) Subcellular localization of Pi05910-GFP (upper panel and middle panel) and Pi05910-GFP$_{NES}$ (bottom panel) in *Nicotiana benthamiana* leaves. The constructs *35S::Pi05910-GFP* and *35S::Pi05910-GFP$_{NES}$* were transiently expressed in *N. benthamiana* leaves by agroinfiltration for 2 days. UGP1-mCherry and 4′,6-diamidino-2-phenylindole (DAPI) are cytoplasmic and nuclear markers, respectively. Scale bars: 20 μm. Grey value plot shows the relative fluorescence along the solid line in the images. (b) Nuclear localization of Pi05910 is required for its virulence functions. *Pi05910-GFP* expression, but not *Pi05910-GFP$_{NES}$*, rendered *N. benthamiana* enhanced susceptibility to *P. infestans*, compared to the negative *FLAG-GFP* control. Representative leaves were stained with trypan blue at 5–7 days post-inoculation (dpi) with *P. infestans* zoospores. Water-soaked lesion diameters of more than 24 leaves were scored and averaged for histogram from three individual experiments. All values were distributed in dots. Statistical analysis was based on Student's *t* test. Asterisks denote statistical significance (**$p < 0.01$; ns, no significance, $p > 0.05$). The error bar represents the standard deviation. Scale bars: 1 cm.

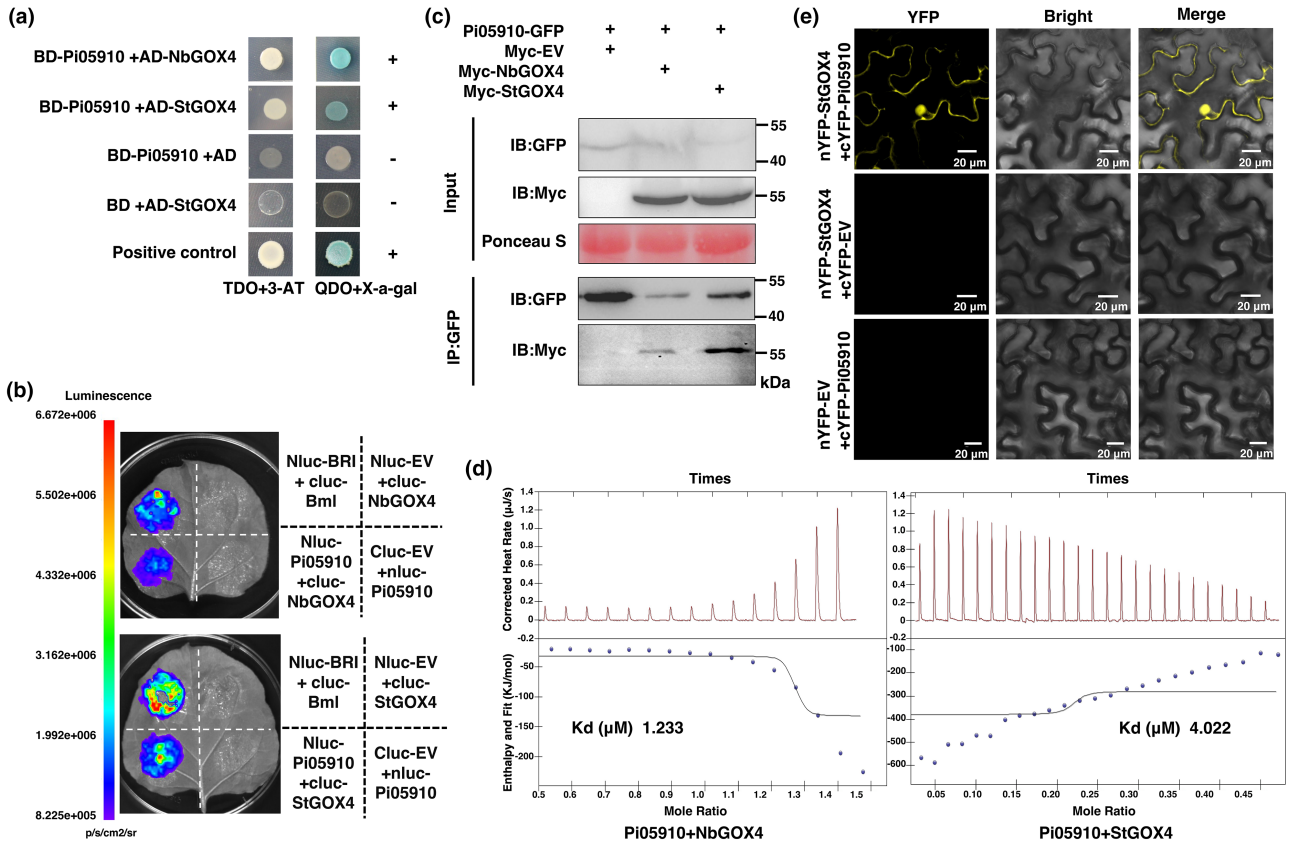

FIGURE 2 Pi05910 interacts with the potato glycolate oxidase protein StGOX4. (a) Yeast cells co-expressing *BD-Pi05910* and *AD-StGOX4/NbGOX4* were grown on triple dropout (TDO; SD/−Leu−Trp−His) + 3-AT medium and yielded X-α-galactosidase activity on quadruple dropout (QDO; SD/−Leu−Trp−His−Ade). +, protein interaction in yeast two-hybrid assay. (b) Luciferase complementation imaging analysis showed the interaction between Nluc-Pi05910 and Cluc-StGOX4 or NbGOX4 in planta, with the combination of Nluc-BRI with Cluc-Bml used as positive control. (c) Co-immunoprecipitation confirmed Pi05910-GFP interaction with both Myc-NbGOX4 and Myc-StGOX4. Ponceau S verified the equal loading of protein extract. +, confirmed expression of proteins in *N. benthamiana* leaves. (d) In vitro isothermal titration calorimetry analysis showed His-Pi05910 interaction with both His-StGOX4 and NbGOX4. Titrations were done with recombinant Pi05910 and NbGOX4/StGOX4 protein solutions in sample cell. The upper panel shows the heat rate to titrations, and the bottom panel shows the integrated heat effect value fitted to a single-site model. (e) Bimolecular fluorescence complementation assay confirmed Pi05910 interaction with StGOX4 in the nucleus and cytoplasm. *nYFP-StGOX4* was co-expressed with *cYFP-Pi05910* in *N. benthamiana* leaves for 2 days. YFP fluorescence (514 nm excitation) was observed by confocal laser microscopy. Scale bars: 20 μm.

and no transformants were obtained, which suggests that silencing *StGOX4* is probably lethal.

Heterologous expression of *35S::GFP-StGOX4* in *N. benthamiana* by agroinfiltration followed by *P. infestans* infection produced significantly smaller lesions compared with *FLAG-GFP*. The expression and integrity of GFP-StGOX4 and FLAG-GFP proteins were confirmed by western blotting (Figure 3b, Figure S7c). Transient expression of *35S::GFP-NbGOX4* in *N. benthamiana* showed immune function consistent with that of *35S::GFP-StGOX4* (Figure 3c, Figure S7d). In addition, a 280 bp fragment (644–923 bp) was selected to prepare *NbGOX4*-silenced plants (TRV-*NbGOX4*) by virus-induced gene silencing (VIGS) (Figure S7e) and the relative transcript level of *NbGOX4* was quantified by RT-qPCR (Figure S7f). Silencing of *NbGOX4* rendered plants chlorotic and dwarf (Figure S7g). Infection assays showed significantly larger lesions on *NbGOX4*-silenced detached leaves compared with the TRV-*GFP* control, confirming that *NbGOX4*-silencing significantly enhanced plant susceptibility to *P. infestans* (Figure 3d). In conclusion, StGOX4 and NbGOX4 share a conserved immune function in resistance to *P. infestans*.

To investigate which subcellular localization of StGOX4 is required for resistance function, a nuclear localization signal (NLS) and a nuclear export signal (NES) were fused to the N-terminus of GFP-StGOX4 to make constructs *35S::*$_{NLS}$*GFP-StGOX4* and *35S::*$_{NES}$*GFP-StGOX4*, respectively. We transiently expressed *35S::*$_{NLS}$*GFP-StGOX4* and *35S::*$_{NES}$*GFP-StGOX4* in *N. benthamiana* leaves, followed by confocal microscopy observation. The results showed that the NES signal targeted GFP-StGOX4 outside the nucleus, and GFP-StGOX4 with the NLS signal mainly accumulated inside the nucleus, as expected (Figure 3e). Infection assays showed that overexpression of $_{NLS}$*GFP-StGOX4* or $_{NES}$*GFP-StGOX4* enhanced plant resistance to *P. infestans* colonization (Figure 3f,g). To test whether the nuclear localization of StGOX4 protein is crucial for its interaction with Pi05910, we transiently expressed *35S::*$_{NLS}$*GFP-StGOX4* and *35S::*$_{NES}$*GFP-StGOX4* with *35S::Pi05910-mCherry* in leaves of *N. benthamiana*. The

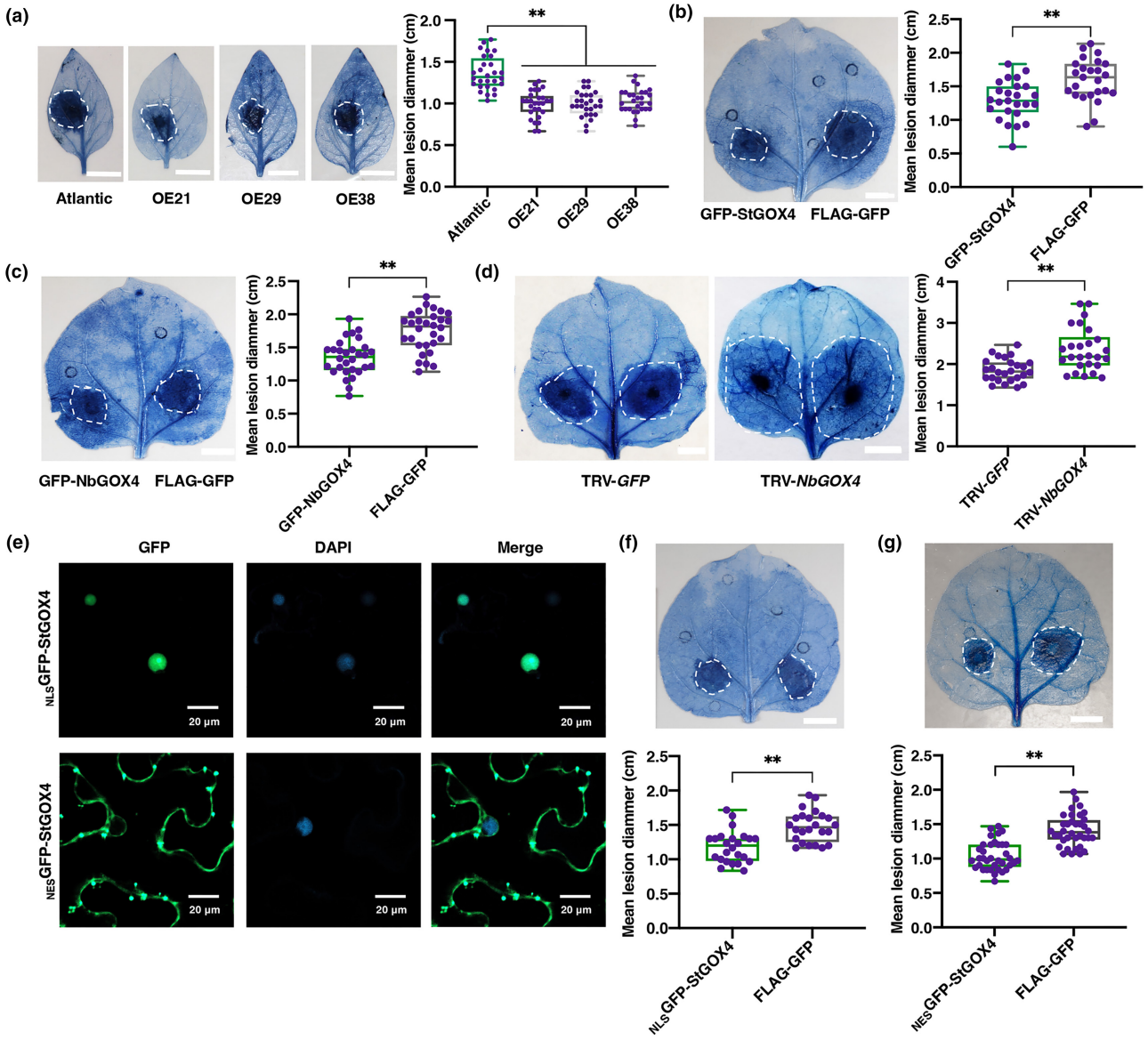

FIGURE 3 *StGOX4* enhances plant resistance to *Phytophthora infestans*. (a) Trypan blue staining to show lesion sizes of potato overexpression lines OE-*StGOX4* and Atlantic upon inoculation with *P. infestans* zoospores after 4 days. (b–d) Trypan blue staining to show the lesion area of *Nicotiana benthamiana* transiently overexpressing *GFP-StGOX4* (b) or *GFP-NbGOX4* (c), and *NbGOX4*-silenced plants (d) upon inoculation with *P. infestans* after 6 days. (e) Subcellular localization of $_{NLS}$GFP-StGOX4 and $_{NES}$GFP-StGOX4. Scale bars: 20 μm. (f, g) Trypan blue staining to show *P. infestans* lesions following transient expression of *35S::*$_{NLS}$*GFP-StGOX4* (f) and *35S::* $_{NES}$*GFP-StGOX4* (g) in *N. benthamiana* leaves. Water-soaked lesion diameters of more than 24 leaves were scored and averaged for histogram from three individual experiments. All values were distributed in dots. Statistical analysis was based on Student's *t* test. Asterisks denote statistical significance (**$p < 0.01$). The error bar represents the standard deviation. Scale bars: 1 cm.

results indicated that the change of StGOX4 nuclear localization did not affect StGOX4 binding by Pi05910 (Figure S8).

2.4 | ROS burst is involved in the *StGOX4*-mediated resistance to *P. infestans*

GOX has been shown to play roles in ROS and SA responses (Ahammed et al., 2018). Because GOX produces H_2O_2 in the photorespiratory pathway (Liu et al., 2018), to reveal the role of GOX in the ROS burst in the peroxisome, we expressed peroxisome targeting redox-sensitive GFP (RoGFP2-SKL) (Cao et al., 2024) to observe the redox status in *NbGOX4*-silenced plants. RoGFP2-SKL with a smaller ratio of 405 nm:488 nm fluorescence intensity in TRV-*NbGOX4* indicates less ROS accumulated (Figure S9a). To further investigate whether NbGOX4 affects ROS levels in other photorespiration-related organelles, we stained the TRV-*GFP* and TRV-*NbGOX4* leaves with a ROS fluorescence probe (CM-H_2DCFDA) (Yang et al., 2022) and found significantly reduced ROS levels in *NbGOX4*-silenced plants, especially in the nucleus and chloroplast (Figure S9b). Furthermore,

we measured the redox changes in the nucleus by using the modified RoGFP2 (Waypa et al., 2010) biosensor, by fusing an NLS signal to its N-terminus (*35S::NLS-RoGFP2*). Fluorescence was observed after transient expression of *35S::NLS-RoGFP2* in TRV-*GFP* and TRV-*NbGOX4* plants after 3 days. *NLS-RoGFP2* expression with a smaller ratio of 405 nm:488 nm fluorescence intensity indicated decreased oxidative stress in TRV-*NbGOX4* plants. The results showed that ROS signals in the nucleus decreased significantly in the *NbGOX4*-silenced leaves (Figure 4a).

We further examined whether silencing *GOX* led to an alteration in the *P. infestans*-associated ROS burst, by inoculating TRV-*GFP* and TRV-*NbGOX4* plants with *P. infestans*. The leaves were treated with 3,3′-diaminobenzidine tetramine hydrochloride (DAB) to examine H_2O_2 at 5 days post-inoculation (dpi). The results showed that ROS accumulation was significantly reduced in the *NbGOX4*-silenced plants (Figure 4b,c). DAB staining and H_2O_2 quantification also showed that overexpression of *GFP-StGOX4* led to significantly higher levels of ROS compared to the *FLAG-GFP* plants 24 h post-inoculation (hpi) upon *P. infestans* infection (Figure S9c). Similar results were obtained for potato *StGOX4* transformants OE21, OE29 and OE38 (Figure S9d).

To further explore whether *NbGOX4* is involved in ROS and SA signalling pathways, the expression of marker genes at different time points of *P. infestans* infection was monitored in *NbGOX4*-silenced plants. *NbPR1* and *NbPR5* are marker genes in the SA signalling pathway (Wang et al., 2023), while *NbBIK1*, *NbSIK1*, *NbRBOHD* and *NbEX1* are markers of ROS pathways, functioning in ROS perception, response, activation and photosystem II (PSII) signalling pathways (Li et al., 2014, 2024; Zhang, 2020; Zhang et al., 2018). RT-qPCR results showed that silencing *NbGOX4* significantly downregulated the expression of *NbSIK1*, *NbBIK1* and *NbRBOHD*, *NbPR1* and *NbPR5* at the late stage of infection and upregulated the expression of *NbEX1* (Figure 4d). Moreover, the expression of *StPR1* and *StPR5* was also significantly upregulated in potato OE-*StGOX4* lines at the late stage of infection (Figure S9e).

Taken together, these results indicate that *StGOX4* plays a regulatory role in the defence responses related to ROS and SA signalling pathways.

2.5 | Pi05910 inhibits the enzymatic activity of StGOX4

To examine the enzymatic properties of StGOX4, glycolate, L-lactate and D-lactate were selected as substrates (Schmitz et al., 2020). The enzymatic activity of recombinant StGOX4 protein was highest when glycolate was used as a substrate, followed by L-lactate, but was not detectable with D-lactate (Figure 5a). Glycolate was therefore chosen as the preferred substrate for further analyses. Co-incubation of His-StGOX4 with recombinant His-Pi05910 led to significantly reduced StGOX4 activity (Figure 5b). We examined in vivo enzymatic activity of StGOX4 by transient *35S::Myc-StGOX4* overexpression in *N. benthamiana* followed quantitative analyses of the absorbance values, which were significantly reduced when *35S::Pi05910-GFP* was co-expressed compared to the co-expression with *35S::FLAG-GFP* (Figure 5c). In order to explore whether StGOX4 has enzymatic activity in the nucleus, we extracted nuclear proteins from plants co-expressing *Myc-StGOX4* and *Pi05910-GFP* and examined the enzymatic activity. Although the enzymatic activity of StGOX4 in the nucleus decreased, Pi05910 could still significantly reduce the activity of StGOX4 (Figure 5d). We co-expressed $_{NLS}$*GFP-StGOX4* and $_{NES}$*GFP-StGOX4* with *Pi05910-mCherry* to explore the effect of Pi05910 on StGOX4 enzymatic activity. The Pi05910-mediated inhibition of StGOX4 enzymatic activity functioned both inside and outside the nucleus (Figure S10). These results demonstrated that Pi05910 inhibits the enzymatic activity of StGOX4.

2.6 | The Tyr-25 residue of StGOX4 is required for Pi05910 interaction and immunity

The crystal structure of spinach GOX was resolved in 1985 (Lindqvist & Branden, 1985). Protein sequence analysis of StGOX4 using ExPasy (https://www.expasy.org/resources/scanprosite) identified four amino acid residues (Y25, Y130, R165 and R258) related to substrate binding and four residues (S107, Q128, T156 and K231) related to FMN binding (Figure S11). To examine whether the active sites of StGOX4 are required for its interaction with Pi05910, a mutant with all substrate-binding residues converted into alanine was generated as M(S), while a mutant of all FMN-binding residues was created and designated as M(F). As Tyr25 was found to be one of the key active residues of the substrate bound of spinach GOX (Cunane et al., 2005), we generated mutant M1 where Y25 was changed to alanine (Figure 5e). Co-IP assays showed that mutants M(S) and M1 lost ability to interact with Pi05910, while mutant M(F) remained capability to interact with the effector (Figure 5f). These results showed that substrate binding, but not FMN binding, was important to its interaction with Pi05910. The Y25 residue is a key for the StGOX4 interaction with Pi05910.

To examine whether these mutations had abolished enzymatic activity, we purified recombinant His-M(S), His-M(F) and His-M1 and determined that all mutants showed no detectable enzymatic activity compared with the wild-type StGOX4 (Figure S12). To investigate whether the predicted enzymatic activity of StGOX4 is required for its positive role in plant defence, a *P. infestans* infection assay was conducted after agroinfiltration-mediated transient expression of the *StGOX4* mutants. The mutants M(S) and M(F) increased susceptibility of plants to *P. infestans*, whereas mutant M1 lost its ability to increase resistance (Figure 5g). Western blotting confirmed the expression and integrity of the mutant proteins (Figure S13). Thus, the enzymatic activity of StGOX4 is required for its immune function and the Y25 residue is required for the ability of StGOX4 to mediate plant immunity to *P. infestans* infection.

Taken together, these results suggest that the Y25 residue is critical for enzymatic activity and binding with Pi05910 and plays a key role in its positive regulation of immune responses.

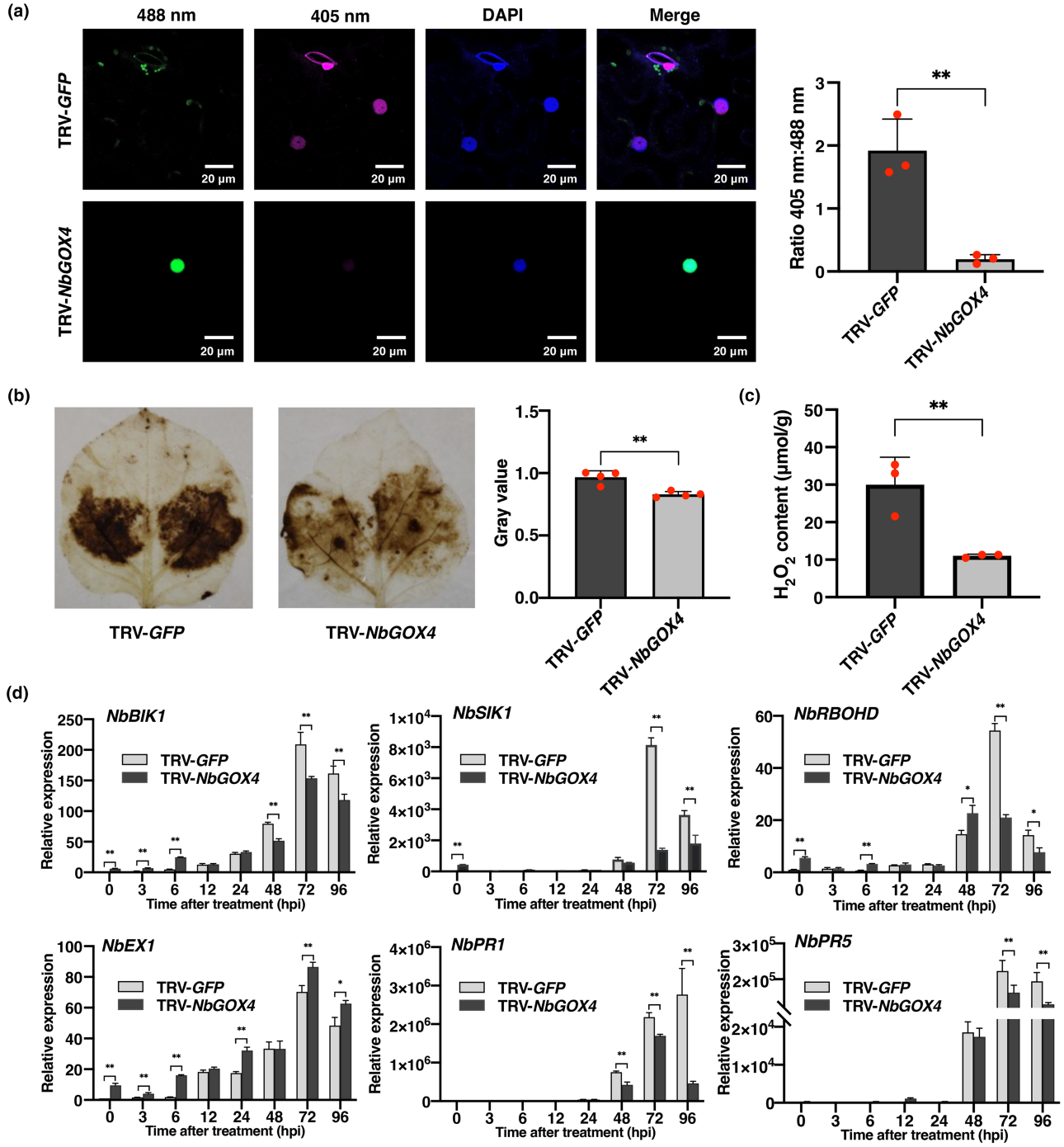

FIGURE 4 *NbGOX4*-silencing suppresses reactive oxygen species (ROS) and salicylic acid (SA) signalling pathways. (a) The biosensor construct *35S::NLS-RoGFP2* was transiently expressed in TRV-*GFP* and TRV-*NbGOX4* plants, observed with laser scanning microscopy. Scale bars: 20 μm. The fluorescence intensity ratio of the *NLS-RoGFP2* biosensor [405 nm:488 nm] was used to detect the dynamic redox environment in the nucleus. Fluorescence intensity ratio 405 nm:488 nm of TRV-*GFP* leaves was set to 1. Statistical analysis was based on Student's *t* test. Asterisks denote statistical significance (**$p < 0.01$). Three values were distributed in dots. The error bar represents the standard deviation of three independent biological replicates. (b) 3,3′-diaminobenzidine (DAB) staining showed less ROS accumulation in TRV-*NbGOX4* leaves. DAB staining grey value of TRV-*GFP* leaves was set to 1. Four values were distributed in dots. The error bar represents the standard deviation of four independent biological replicates. (c) H_2O_2 content was detected in TRV-*GFP* and TRV-*NbGOX4* leaves inoculated with *Phytophthora infestans*. The red dots in the figure indicate the specific quantities of H_2O_2. (d) Reverse transcription-quantitative PCR (RT-qPCR) data showing relative expression of the ROS marker genes *NbBIK1*, *NbSIK1*, *NbRBOHD* and *NbEX1*, and the SA-responsive genes *NbPR1* and *NbPR5* in TRV-*GFP* and TRV-*NbGOX4* plants. *NbActin* gene expression was used for normalization in RT-qPCR assays. Statistical analysis based on Student's *t* test. Asterisks denote statistical significance (**$p < 0.01$). The error bar represents the standard deviation. Similar results were obtained for three individual experiments.

2.7 | Pi05910 binding destabilizes StGOX4

To investigate the impact of Pi05910 on StGOX4, we co-expressed *35S::Pi05910-GFP* and *35S::Myc-StGOX4* in *N. benthamiana* leaves and examined StGOX4 protein accumulation. Significantly decreased StGOX4 accumulation was notable in the presence of Pi05910 compared with FLAG-GFP (Figure 6a). We then examined whether Pi05910 destabilizes StGOX4 in 26S proteasome- or autophagy-dependent pathways. The 26S proteasome inhibitor MG132 or autophagy inhibitor 3-methyladenine (3-MA), with its solvent dimethyl sulphoxide (DMSO) as a negative control, was infiltrated at 36 h post-agroinfiltration of bacteria carrying *35S::Myc-StGOX4* with *35S::FLAG-GFP* or *35S::Pi05910-GFP*. No significant difference was notable in the abundance of StGOX4 after MG132 or 3-MA treatment when co-expressed with *35S::Pi05910-GFP* or *35S::FLAG-GFP* (Figure 6b), suggesting that Pi05910 might decrease StGOX4 accumulation independent of 26S proteasome- and autophagy-mediated degradation.

3 | DISCUSSION

Pathogens encode numerous secreted effector proteins that play important roles in mediating plant–pathogen interactions, frequently manipulating plant immunity in favour of pathogen infection (Fabro, 2022). In this study, we focused on *P. infestans* Pi05910, an RXLR effector conserved and highly expressed at early stage of infection by *P. infestans* (Yin et al., 2017). We showed that it has potato genotype-specific elicitor function in potato cultivar Longshu 12 (Figure S1). To understand how Pi05910 manipulates host immunity in the absence of a cognate resistance gene, we determined that it enhanced susceptibility in *N. benthamiana* to *P. infestans* (Figure 1b). We found that Pi05910 interacted with glycolate oxidase NbGOX4 and its orthologue protein StGOX4 in potato using multiple experimental approaches, including Y2H, LCI, Co-IP and ITC assays (Figure 2). Our results provide a new perspective on the virulence mechanism of Pi05910.

Plant GOXs have been reported to be conserved and functionally diverse in plant–pathogen interactions (Dong et al., 2023; Schmitz et al., 2020). We showed that StGOX4 and NbGOX4 are positive regulators of plant immunity in potato and *N. benthamiana*, respectively (Figure 3a–d). GOX regulates plant responses to stress mainly through H_2O_2 (Schmitz et al., 2020; Xu et al., 2018; Yang et al., 2018) and SA. Our results showed that the ROS levels in *NbGOX4*-silenced plants were significantly reduced but significantly increased in *StGOX4*-overexpressing lines. Furthermore, TRV-*NbGOX4* plants showed decreased expression levels of SA signalling markers *NbPR1* and *NbPR5*, while *StGOX4*-overexpressing lines showed higher transcript levels of *StPR1* and *StPR5* (Figure 4, Figure S9). These results suggest that StGOX4 positively regulates plant immunity to *P. infestans* by promoting ROS and SA signalling. The specific mechanism of Pi05910 on ROS and SA signalling pathways needs to be further studied.

GOX acts as an α-hydroxyl acid oxidase and is involved in cell oxidation, acid metabolism, stress response and other cellular processes (Foyer et al., 2009; Schmitz et al., 2020). Pathogen effectors are known to interfere with the enzymatic activity of host target proteins (Fan et al., 2018; Lin et al., 2021; Sun et al., 2017). Here, the enzyme coupling assays showed that StGOX4 catalyses glycolate oxidation with the highest enzymatic activity with glycolate as the substrate, and effector protein Pi05910 inhibited the enzymatic activity of StGOX4 both in vivo and in vitro (Figure 5a–c), indicating that Pi05910 directly inhibits StGOX4 enzymatic activity. A truncation assay of OsGOX1 in rice showed that there may be key amino acids interacting with OsCATC in the non-active central region (Li, 2017), which is of great significance for understanding the mechanism of plant response to stress. However, the mechanism of the active site of StGOX4 in the plant response to *P. infestans* infection remains to be studied. In this study, we found that the Y25 residue of StGOX4 is required for Pi05910 interaction and is crucial for resistance to *P. infestans* (Figure 5d–f), illustrating the importance of the Y25 residue in plant–pathogen interactions.

The GOX family protein sequences contain a tripeptide PTS1 that determines the peroxisome localization of the GOX family proteins (Reumann et al., 2012). We found that StGOX4 localized in the nucleus, cytoplasm and peroxisomes (Figure S5). Our finding is incongruent with previous reported localization. One possible explanation could be the short peptide motif upstream of the PTS1 domain leads to other subcellular localizations of proteins located in the peroxisome (Deng et al., 2022). The peroxisome-localized CAT protein contains a peroxisome-targeting peptide and is capable of being transported to the nucleus without the influence of exogenous proteins (Baker et al., 2023). We confirmed the presence of full-length GFP-StGOX4 protein in the nucleus (Figure S5a) and that StGOX4 has enzymatic activity in the nucleus (Figure 5d, Figure S10a). Further studies are warranted to dissect the nuclear localization of StGOX4. Our work revealed that Pi05910 localizes to the nucleus and cytoplasm and that nuclear localization is required for its virulence function (Figure 1). However, the interaction between Pi05910 and StGOX4 or the inhibition of Pi05910 on StGOX4 enzymatic activity can occur in both nucleus and cytoplasm (Figure 2e, Figures S8 and S10). There might be other unclear mechanisms, such as targeting additional host cell components, that are not accessible in the cytoplasm. Many *Phytophthora* effectors target multiple host cell components to suppress host immunity (Bos et al., 2010; Chaparro-Garcia et al., 2015; Li et al., 2019).

Pathogen effectors degrade or stabilize target proteins to suppress host immunity. *P. sojae* CRN78 degrades NbPIP2;2 or GmPIP2-13 in the 26S-dependent pathway to suppress immunity (Ai et al., 2021). *P. infestans* RXLR effector Pi06432 targets and stabilizes StUDP to degrade StRPT3b via the 26S proteasome and autophagy pathways (Wang et al., 2023). Our data showed that Pi05910 destabilizes StGOX4 in a manner independent of the 26S proteasome- or autophagy-mediated pathways (Figure 6a,b). Overexpression of midnolin causes the nucleoprotein to degrade its target without the need for ubiquitination (Gu et al., 2023), which is one of the possible

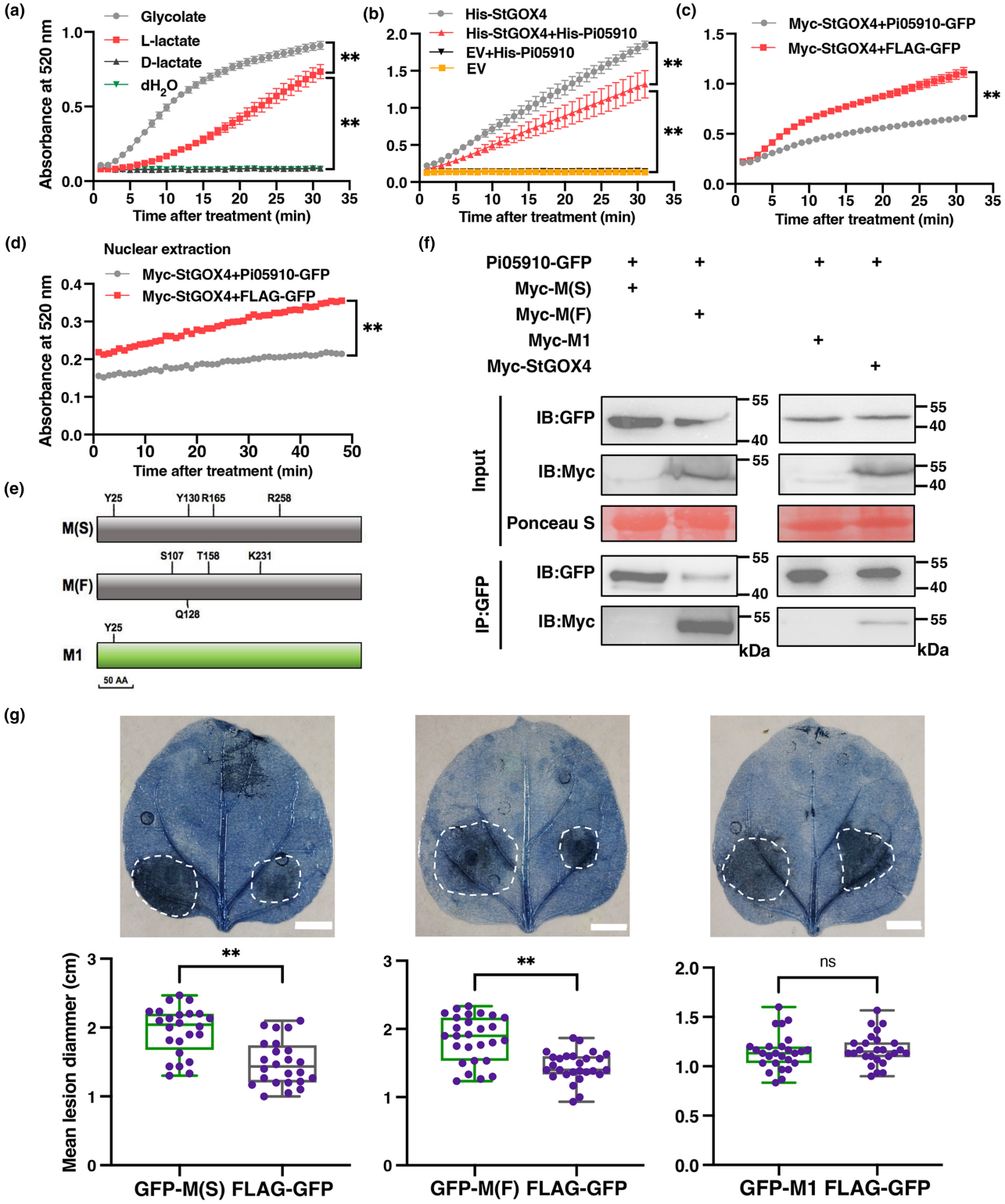

reasons for Pi05910 to target and degrade StGOX4. Alternatively, crystal structure analysis revealed a difference of substrate-binding sites in GOX and HAOX or the active sites affecting flavin orientation in animals due to tyrosine replacement by phenylalanine (Y25 of StGOX4) (Cunane et al., 2005), suggesting a critical residue it shares. We speculate that the interaction between Pi05910 and StGOX4 via the Y25 residue might change the conformation of StGOX4, thereby reducing its stability. The mechanism by which effector protein Pi05910 affects the stability of StGOX4 needs to be further studied.

In summary, we found that the conserved RXLR effector Pi05910 of *P. infestans* targets StGOX4, a positive immune regulator that involves the ROS and SA signalling pathways. Pi05910 suppresses plant immune responses by inhibiting enzymatic activity and stability of StGOX4. Further understanding of Pi05910-mediated immune

FIGURE 5 Tyr-25 residue is required for StGOX4 immune function and mediates its interaction with Pi05910. (a) Glycolate oxidase activity was analysed using glycolate, l-lactate and d-lactate as substrates by in vitro horseradish peroxidase coupling method. The recombinant protein His-StGOX4 was expressed and purified in *Escherichia coli* BL21(DE3). The absorbance at 520 nm indicates enzymatic activity of StGOX4. (b) The purified 0.5 mM His-StGOX4 was incubated with 0.5 mM His-Pi05910; enzymatic activities were detected with glycolate as substrate. Crude enzyme solutions (c) and nuclear proteins (d) were extracted from *35S::Pi05910-GFP/35S::FLAG-GFP* transiently co-expressed with *35S::Myc-StGOX4* in *Nicotiana benthamiana* leaves; enzymatic activities were subsequently detected. (a–d) Each data point comprises three replicates. The error bar represents the standard deviation. Statistical analysis was based on Student's *t* test. Asterisks denote significant difference (**$p < 0.01$). Similar results were obtained for three individual experiments. (e) Schematic diagrams of StGOX4 enzymatic active mutants. The residues indicated in the diagram were all mutated to alanine to generate specific mutants. (f) *35S::Pi05910-GFP* was co-expressed with *35S::Myc-StGOX4*, *35S::Myc-M1*, *35S::Myc-M(S)*, *35S::Myc-M(F)*. Co-immunoprecipitation was performed with GFP beads. +, confirmed expression of proteins in the leaves. (g) Immune function analysis of *StGOX4* mutants. *StGOX4* mutants driven by the 35S promoter and *35S::FLAG-GFP* were transiently expressed in *N. benthamiana* leaves upon inoculation with *Phytophthora infestans* zoospores. The white dashed circle shows lesion area. Scale bars: 1 cm. The error bar represents the standard deviation. Lesion diameters of more than 24 leaves were scored and averaged for histogram from three individual experiments. All values were distributed in dots. Statistical analysis was based on Student's *t* test. Asterisks denote significant difference (**$p < 0.01$; ns, no significance, $p > 0.05$).

suppression will facilitate development of new strategies to improve crop disease resistance.

4 | EXPERIMENTAL PROCEDURES

4.1 | Culture of strains and plants

Escherichia coli DH5α was used for plasmid extraction, and *E. coli* BL21(DE3) was used for protein purification experiment. *Agrobacterium tumefaciens* GV3101 and AGL1 were used for transient expression, stable transformation and VIGS expression. *E. coli* and *A. tumefaciens* were routinely cultured in Luria Bertani (LB) agar with different antibiotics at 37°C and 28°C, respectively. *Saccharomyces cerevisiae* AH109 was used in yeast-two-hybrid assay. Zoospores of *P. infestans* 88069 were prepared for inoculation. *N. benthamiana* and potato were grown in a climate-controlled greenhouse (23°C, 13 h light/11 h dark).

4.2 | Plasmid construction

GOX4 genes were cloned from *N. benthamiana* and potato cultivar Longshu 12. All sequences were amplified by FastPfu DNA polymerase (Transgene Biotech) and cloned into the pART27, pART27-CGFP (Gleave, 1992), pART27-NGFP (Zhang et al., 2021), pART27-Nmyc (Fan et al., 2018) or pART27-Nmyc-mCherry vectors under the transcriptional control of the CaMV 35S promoter, which were used for overexpression experiments. For overexpression vectors, coding sequences were inserted between the XhoI (New England Biolabs) and XbaI sites or cloned between the XhoI and EcoRI sites or cloned between the EcoRI and XbaI sites. The modified redox-sensitive GFP was as described (Waypa et al., 2010) and was fused with NLS at its N-terminus (*NLS-RoGFP2*). The fusion construct was inserted into the XhoI and XbaI sites of pART27 vector. For Y2H assay, the *Pi05910* coding sequence was cloned into pGBKT7 while *GOX4* into pGADT7 between the EcoRI and BamHI sites. For BiFC assay, *StGOX4* was cloned into the StuI and KpnI sites of pDEST-VYNE(R) Gateway vector to form the *nYFP-StGOX4* plasmid. *Pi05910* was cloned into the SpeI and XhoI sites of pDEST-VYCE(R) Gateway vector to form the *cYFP-Pi05910* plasmid. To generate VIGS constructs, a 280 bp fragment of *NbGOX4* was cloned into the EcoRI and BamHI sites of binary vector pTRV2, while TRV2-*GFP* was constructed as a control. For LCI assay, *Pi05910* was cloned into pCAMBIA1300-Nluc while *GOX4* into pCAMBIA1300-Cluc between the KpnI and SalI sites. For protein purification, all proteins were inserted using NcoI and XhoI sites into the pET-32a vector. Ligations were performed using MonClone Single Assembly Cloning Mix (Monad) or T4 DNA ligase (Thermo Scientific). All constructs were sequenced at Tsingke (Beijing, China). All primers used for plasmid constructions are listed in Table S2.

4.3 | Agroinfiltration-mediated transient expression

Agrobacterium tumefaciens GV3101 or AGL1 carrying respective constructs were centrifuged at 4000 *g* for 5 min to collect agrobacteria and suspended in MES buffer with 100 μM acetosyringone. The concentration of agrobacterial suspension was measured by spectrophotometer, and OD_{600} value was adjusted to 0.2–0.8. A needleless syringe was used to inject from the flat area between the veins on the back of the leaf (Elnahal et al., 2020; Meng et al., 2015).

4.4 | Confocal microscopy

The fused proteins with different fluorescent labels and reagent were transiently expressed in *N. benthamiana* for BiFC and subcellular localization assays. The excitation and emission wavelengths of each fluorescent label are described previously (Du et al., 2021). An LSM900 laser scanning microscope (Zeiss) or FV3000 confocal microscope (Olympus) was used for initial

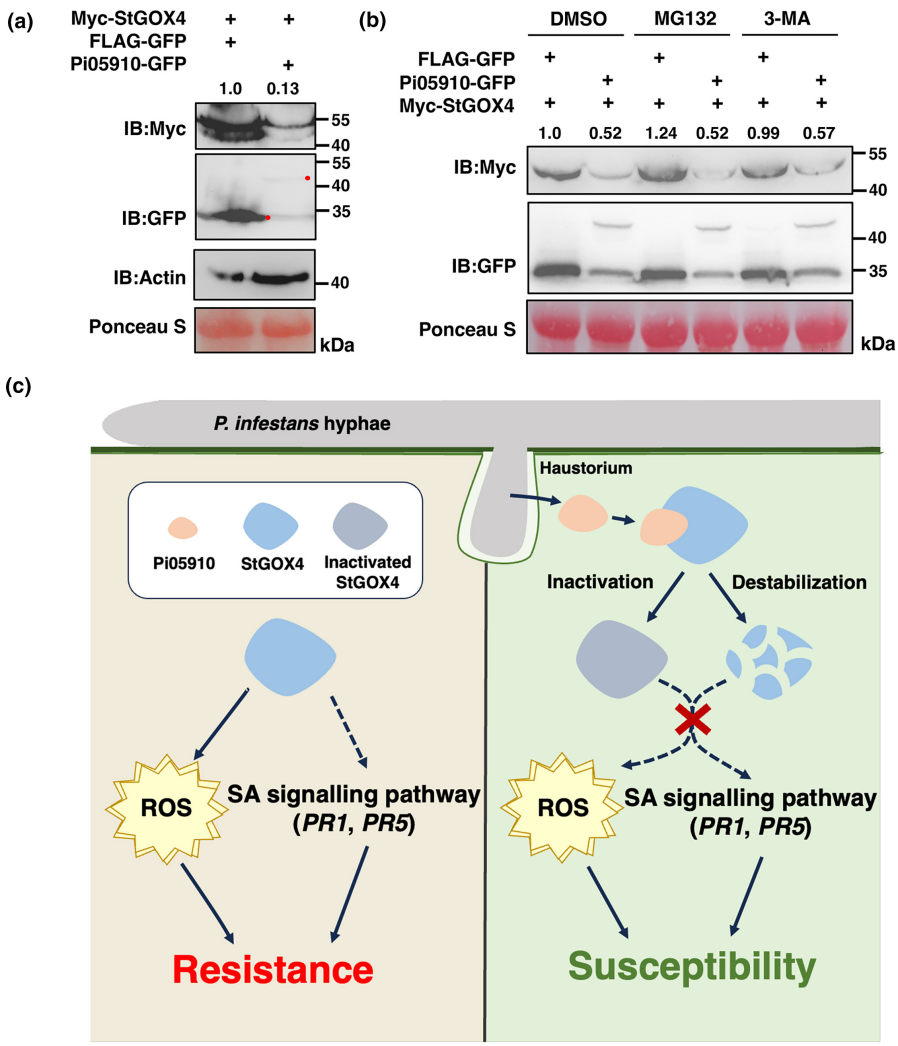

FIGURE 6 Pi05910 destabilizes StGOX4. (a) Western blotting showed the accumulation of Pi05910-GFP and FLAG-GFP proteins co-expressed with Myc-StGOX4 in *Nicotiana benthamiana*. Proteins were extracted at 2 days after agroinfiltration. The red dots indicate the corresponding protein bands. NbActin was used as internal reference protein. (b) *35S::Pi05910-GFP* or *35S::FLAG-GFP* was co-expressed with *35S::Myc-StGOX4* in *N. benthamiana* leaves, followed by infiltration with MG132, 3-methyladenine (3-MA) or dimethyl sulphoxide (DMSO) after 36 h. Proteins were extracted at 12 h following treatments with MG132, 3-MA or DMSO. +, confirmed expression of proteins in the leaves. Protein equal loading is indicated by Ponceau S staining. The calculated grey value of ImageJ is indicated above the bands. (c) Proposed model of immune suppression mechanisms induced by Pi05910 targeting of host glycolate oxidase4 (StGOX4) during infection. In the early stage of infection, *Phytophthora infestans* effector Pi05910 targets host StGOX4, a positive regulator of plant immunity, leading to inhibition of its enzymatic activity and stability to render plant susceptibility. *StGOX4* positively regulates plant immunity by enhancing reactive oxygen species (ROS) accumulation and activating salicylic acid (SA) signalling pathway.

observation and image acquisition. Fluorescent intensities were examined using ImageJ software by determining the grey value. DAPI (4′,6-diamidino-2-phenylindole) is a nuclear fluorescent dye with blue divergent light (Linhoff et al., 2015). DAPI (100 ng/mL) was infiltrated into *N. benthamiana* leaves 15–30 min before confocal observation. H4-mCherry was used as nuclear marker (Zhong et al., 2022), UGP1-mCherry as a cytoplasmic marker (Furtauer et al., 2019) and PTS2-mCherry as a peroxisome marker (Kunze, 2020). CM-H_2DCFDA was used to detect ROS (Yang et al., 2022). *NLS-RoGFP2* and *RoGFP2-SKL* (Cao et al., 2024) were excited by 405 and 488 nm lasers, respectively. The fluorescence intensity ratio of 405 nm:488 nm was calculated.

4.5 | Inoculation of the detached leaves with *P. infestans*

To prepare zoospores, *P. infestans* 88069 was cultured on solid rye medium at 16°C for 10–15 days, followed by flooding with 4–5 mL of precooled sterile distilled water. The plates were incubated for 1–2 h in a refrigerator at 4°C to fully release zoospores.

To perform infection assays on *N. benthamiana* leaves, about 1000 *P. infestans* zoospores were drop-inoculated on detached leaves and placed in a dark incubator at 16°C. After 5–7 days, the lesion diameters were measured following trypan blue staining. To infect potato leaves, about 500 *P. infestans* zoospores were

drop-inoculated on potato leaves and placed in a dark incubator at 16°C, and the lesion was scored as described above after 3 days.

4.6 | Luciferase complementation imaging assay

The fusion protein constructs in pCAMBIA1300-Nluc and pCAMBIA1300-Cluc were co-expressed on *N. benthamiana*. The modules Nluc and Cluc were close enough in space to perform the fluorescein enzymatic activity. A small amount of luciferase was applied to the injection area and placed in the dark for 5 min. The images were collected by multispectral dynamic fluorescence microscopy (CCD). The combination of Nluc-BRI with Cluc-Bml was used as positive control (Zhang, 2019).

4.7 | Yeast-two-hybrid assay

The plasmid BD and AD constructs were co-transformed into *S. cerevisiae* AH109. The transformants were grown on SD/−Leu−Trp agar medium for 3 days and then were selected normally on TDO (SD/−Leu−Trp−His) + 3-AT and turn blue on QDO (SD/−Leu−Trp−His−Ade) + X-α-gal, which proved the interaction between proteins. Y2H screening was performed using the Matchmaker Gal4 Two-Hybrid System 3 (Clontech) as described in the manual (Li et al., 2022).

4.8 | Co-immunoprecipitation assay and Western blotting

To extract proteins, plant leaves were ground in liquid nitrogen into fine powder and extracted by RIP lysis buffer (25 mM Tris pH 7.5, 150 mM NaCl, 1 mM EDTA and 2% wt/vol polyvinylpolypyrrolidone [PVPP], 0.5% NP-40, 1 mM dithiothreitol [DTT], a protease inhibitor cocktail and 1 mM PMSF). GFP-beads (Anti-GFP Affinity Beads 4FF) were used to enrich proteins containing GFP labels. Detailed experimental procedures were described previously (Du et al., 2021). SDS-PAGE followed by western blotting was used to detect protein expression and integrity. Antibodies (anti-Myc, anti-GFP, anti-mCherry, anti-actin, goat anti-mouse, goat anti-rabbit) were from ABclone (Huang et al., 2019). The nuclear proteins were extracted using the plant nuclear protein isolation kit (BestBio).

4.9 | Purification of recombinant proteins

The vector pET-32a-based fusion protein constructs were transformed into *E. coli* BL21(DE3) and cultured at 37°C until OD_{600} of 0.6–0.8. Isopropyl-β-D-thiogalactopyranoside (IPTG) was added and cultured overnight at 120 rpm at 18°C. Protein lysate was suspended and sonicated. His-tag Ni-NTA beads 6FF column was added to the chromatographic column, and the column was successively passed: double distilled water, 10 mM imidazole buffer, protein crude extract, 20 mM imidazole binding buffer, 250 mM imidazole eluent, purified protein was collected. The protein was concentrated with 10 kDa ultrafiltration tube and detected by Coomassie blue staining after SDS-PAGE.

4.10 | Virus-induced gene silencing

A 280 bp sequence from the *NbGOX4* gene was selected to make the TRV-*NbGOX4* plasmid. According to the agroinfiltration conditions (Li et al., 2020), TRV-*PDS* plants were used as indicators to monitor the silencing process, which showed obvious bleaching 3 weeks after agroinfiltration, and the leaf positions of the bleached leaves were selected in our experiment.

4.11 | Enzymatic activity detection

Referring to the reported method of enzyme activity measurement (Xu et al., 2006), enzyme coupling method was used to detect the enzymatic activity of StGOX4. To extract crude enzyme, 0.2 g leaves were ground in precooled 100 mM phosphate-buffered saline (PBS, pH 8.0) and centrifuged at 12000 *g* for 15 min at 4°C. The supernatant was collected and used as crude enzyme solution.

To determine the enzymatic activity, 200 μL reaction system containing 100 mM PBS (pH 8.0), 30 mM 4-amino-antipyrine, 1 mg/mL horseradish peroxidase (POD), 20 mM phenol, 1 mM flavin mononucleotide (FMN), 100 mM substrate and extracted enzyme was used. The mixed solution was added into a transparent plate, and absorbance at 520 nm was measured for 30–50 mins.

4.12 | RNA extraction and RT-qPCR

According to the instructions of Tiangen Reagent kit, total RNA from *N. benthamiana* and potato leaves was extracted. Reverse transcription was performed according to the instructions of PrimeScript RT Master Mix Regent kit (TaKaRa). The obtained cDNA was diluted, and qPCR was performed (Gou et al., 2022). All primers used for RT-qPCR are listed in Table S2.

4.13 | DAB staining and H_2O_2 content measuring

DAB is specific to H_2O_2 and requires peroxidase activity to provide a rapid reaction rate. The detached leaves were inoculated with *P. infestans* zoospores and incubated at 16°C for 6 days before being transferred into DAB solution, wrapped in tin foil and cultured in the dark for 6–8 h. After ethanol decolourization, the images were taken (Zhang et al., 2020).

Changes of H_2O_2 contents in leaves were detected according to the instruction of hydrogen peroxide content detection kit (Solarbio).

4.14 | Transformation of potato

To generate transgenic potato plants, stem segments of cultivar Atlantic were placed on R3B (MS-519, sucrose, agar, 1-naphthaleneacetic acid, 6-benzylaminopurine, pH 5.8) medium, treated with PACM (MS-519, sucrose, casein hydrolysate, 2,4-D, kinetin, pH 6.5) for 24 h, followed by agroinfiltration with *A. tumefaciens* GV3101 suspension and transfer to the new R3B medium. After 48 h in the dark, the culture was transferred to ZCVK (MS-519, sucrose, agar, zeatin, cefotaxime, vancomycin, kanamycin, pH 5.8) medium until new buds grew. The buds were inserted into MS medium containing kanamycin to select for potential transgenic potato lines (Wang et al., 2023).

4.15 | Statistical analysis

Statistical analysis of gene expression and lesion diameter was based on Student's *t* test. Asterisks indicate significant differences ($^{*}p < 0.05$; $^{**}p < 0.01$; ns, no significance, $p > 0.05$). All data analyses were based on experiments that were repeated at least three times. GraphPad Prism 9 software was used to process data.

ACKNOWLEDGEMENTS

This work was supported by the Key Research and Development Projects of Shaanxi Province (2021LLRH-07), China Agriculture Research System (CARS-09) and the Program of Introducing Talents of Innovative Discipline to Universities from the State of Administration for Foreign Experts Affairs, China (B18042).

DATA AVAILABILITY STATEMENT

The sequences of NbGOX4 and StGOX4 were obtained from the *Nicotiana benthamiana* genome sequence database v1.0.1 at https://solgenomics.net/organism/Nicotiana_benthamiana/genome and the potato genome (PGSC_DM_v3.4_CDS.fasta) database at https://solgenomics.net/organism/Solanum_tuberosum/genome at Sol Genomics Network (https://solgenomics.net), with accession numbers Niben101Scf04174g05001.1 (NbGOX4) and PGSC0003DMT400071115 (StGOX4). Other data that support the findings of this study are available from the corresponding author upon reasonable request.

ORCID

Weixing Shan https://orcid.org/0000-0001-7286-4041

REFERENCES

Ahammed, G.J., Li, X., Zhang, G., Zhang, H., Shi, J., Pan, C. et al. (2018) Tomato photorespiratory glycolate-oxidase-derived H_2O_2 production contributes to basal defence against *Pseudomonas syringae*. *Plant, Cell & Environment*, 41, 1126–1138.

Ai, G., Xia, Q., Song, T., Li, T., Zhu, H., Peng, H. et al. (2021) A *Phytophthora sojae* CRN effector mediates phosphorylation and degradation of plant aquaporin proteins to suppress host immune signaling. *PLoS Pathogens*, 17, e1009388.

Baker, A., Lin, C.C., Lett, C., Karpinska, B., Wright, M.H. & Foyer, C.H. (2023) Catalase: a critical node in the regulation of cell fate. *Free Radical Biology and Medicine*, 199, 56–66.

Bos, J.I., Armstrong, M.R., Gilroy, E.M., Boevink, P.C., Hein, I., Taylor, R.M. et al. (2010) *Phytophthora infestans* effector AVR3a is essential for virulence and manipulates plant immunity by stabilizing host E3 ligase CMPG1. *Proceedings of the National Academy of Sciences of the United States of America*, 107, 9909–9914.

Braet, J., Catteeuw, D. & Van Damme, P. (2022) Recent advancements in tracking bacterial effector protein translocation. *Microorganisms*, 10, 260.

Cabre, L., Jing, L., Makechemu, M., Heluin, K., El Khamlichi, S., Leprince, J. et al. (2024) Additive and specific effects of elicitor treatments on the metabolic profile of *Arabidopsis thaliana*. *Molecular Plant–Microbe Interactions*, 37, 112–126.

Cao, Y., Zhang, Q., Liu, Y., Yan, T., Ding, L., Yang, Y. et al. (2024) The RXLR effector PpE18 of *Phytophthora parasitica* is a virulence factor and suppresses peroxisome membrane-associated ascorbate peroxidase NbAPX3-1-mediated plant immunity. *New Phytologist*, 243, 1472–1489.

Chaparro-Garcia, A., Schwizer, S., Sklenar, J., Yoshida, K., Petre, B., Bos, J.I.B. et al. (2015) *Phytophthora infestans* RXLR-WY effector AVR3a associates with dynamin-related protein 2 required for endocytosis of the plant pattern recognition receptor FLS2. *PLoS One*, 10, e0137071.

Chen, T., Liu, R., Dou, M., Li, M., Li, M., Yin, X. et al. (2020) Insight into function and subcellular localization of *Plasmopara viticola* putative RXLR effectors. *Frontiers in Microbiology*, 11, 692.

Cunane, L.M., Barton, J.D., Chen, Z., Lê, K.H., Amar, D., Lederer, F. et al. (2005) Crystal structure analysis of recombinant rat kidney long chain hydroxy acid oxidase. *Biochemistry*, 44, 1521–1531.

Deng, Q., Li, H., Feng, Y., Xu, R., Li, W., Zhu, R. et al. (2022) Defining upstream enhancing and inhibiting sequence patterns for plant peroxisome targeting signal type 1 using large-scale *in silico* and *in vivo* analyses. *The Plant Journal*, 111, 567–582.

Dewangan, B.P., Gupta, A., Sah, R.K., Das, S., Kumar, S., Bhattacharjee, S. et al. (2023) Xylobiose treatment triggers a defense-related response and alters cell wall composition. *Plant Molecular Biology*, 113, 383–400.

Ding, P. & Ding, Y. (2020) Stories of salicylic acid: a plant defense hormone. *Trends in Plant Science*, 25, 549–565.

Dong, L., Zhang, X., Wang, M., Fu, X., Liu, G. & Zhang, S. (2023) Glycolate oxidase gene family identification and functional analyses in cotton resistance to *Verticillium wilt*. *Genome*, 66, 305–318.

Du, Y., Chen, X., Guo, Y., Zhang, X., Zhang, H., Li, F. et al. (2021) *Phytophthora infestans* RXLR effector PITG20303 targets a potato MKK1 protein to suppress plant immunity. *New Phytologist*, 229, 501–515.

Du, Y., Mpina, M.H., Birch, P.R., Bouwmeester, K. & Govers, F. (2015) *Phytophthora infestans* RXLR effector AVR1 interacts with exocyst component Sec5 to manipulate plant immunity. *Plant Physiology*, 169, 1975–1990.

Elnahal, A.S.M., Li, J., Wang, X., Zhou, C., Wen, G., Wang, J. et al. (2020) Identification of natural resistance mediated by recognition of *Phytophthora infestans* effector gene *Avr3a*^{EM} in potato. *Frontiers in Plant Science*, 11, 919.

Fabro, G. (2022) Oomycete intracellular effectors: specialised weapons targeting strategic plant processes. *New Phytologist*, 233, 1074–1082.

Fan, G., Yang, Y., Li, T., Lu, W., Du, Y., Qiang, X. et al. (2018) A *Phytophthora capsici* RXLR effector targets and inhibits a plant PPIase to suppress endoplasmic reticulum-mediated immunity. *Molecular Plant*, 11, 1067–1083.

Foyer, C.H., Bloom, A.J., Queval, G. & Noctor, G. (2009) Photorespiratory metabolism: genes, mutants, energetics, and redox signaling. *Annual Review of Plant Biology*, 60, 455–484.

Fu, Q., Wang, Y., Yang, J., Jiao, Y., Li, W., Yang, F. et al. (2023) *Plasmopara viticola* RxLR effector PvAvh77 triggers cell death and governs immunity responses in grapevine. *Journal of Experimental Botany*, 74, 2047–2066.

Furtauer, L., Kustner, L., Weckwerth, W., Heyer, A.G. & Nagele, T. (2019) Resolving subcellular plant metabolism. *The Plant Journal*, 100, 438–455.

Garcia, A.G.K. & Steinbrenner, A.D. (2023) Bringing plant immunity to light: a genetically encoded, bioluminescent reporter of pattern-triggered immunity in *Nicotiana benthamiana*. *Molecular Plant–Microbe Interactions*, 36, 139–149.

Giulietti, S., Bigini, V. & Savatin, D.V. (2023) ROS and RNS production, subcellular localization and signaling triggered by immunogenic danger signals. *Journal of Experimental Botany*, 75, 4512–4534.

Gleave, A.P. (1992) A versatile binary vector system with a T-DNA organisational structure conducive to efficient integration of cloned DNA into the plant genome. *Plant Molecular Biology*, 20, 1203–1207.

Gou, X., Zhong, C., Zhang, P., Mi, L., Li, Y., Lu, W. et al. (2022) miR398b and *AtC2GnT* form a negative feedback loop to regulate *Arabidopsis thaliana* resistance against *Phytophthora parasitica*. *The Plant Journal*, 111, 360–373.

Gu, X., Nardone, C., Kamitaki, N., Mao, A., Elledge, S.J. & Greenberg, M.E. (2023) The midnolin-proteasome pathway catches proteins for ubiquitination-independent degradation. *Science*, 381, eadh5021.

Han, Q., Tan, W., Zhao, Y., Yang, F., Yao, X., Lin, H. et al. (2022) Salicylic acid-activated BIN2 phosphorylation of TGA3 promotes *Arabidopsis PR* gene expression and disease resistance. *The EMBO Journal*, 41, e110682.

Han, S., Zhou, X., Shi, L., Zhang, H., Geng, Y., Fang, Y. et al. (2022) *AhNPR3* regulates the expression of *WRKY* and *PR* genes, and mediates the immune response of the peanut (*Arachis hypogaea* L.). *The Plant Journal*, 110, 735–747.

Huang, G., Liu, Z., Gu, B., Zhao, H., Jia, J., Fan, G. et al. (2019) An RXLR effector secreted by *Phytophthora parasitica* is a virulence factor and triggers cell death in various plants. *Molecular Plant Pathology*, 20, 356–371.

Jiang, H., Xia, Y., Zhang, S., Zhang, Z., Feng, H., Zhang, Q. et al. (2023) The CAP superfamily protein PsCAP1 secreted by *Phytophthora* triggers immune responses in *Nicotiana benthamiana* through a leucine-rich repeat receptor-like protein. *New Phytologist*, 240, 784–801.

Jones, J.D.G. & Dangl, J.L. (2006) The plant immune system. *Nature*, 444, 323–329.

Khan, M.N., Siddiqui, M.H., AlSolami, M.A. & Siddiqui, Z.H. (2024) Melatonin-regulated heat shock proteins and mitochondrial ATP synthase induce drought tolerance through sustaining ROS homeostasis in H_2S-dependent manner. *Plant Physiology and Biochemistry*, 206, 108231.

Kunze, M. (2020) The type-2 peroxisomal targeting signal. *Biochimica et Biophysica Acta, Molecular Cell Research*, 1867, 118609.

Launay, A., Jolivet, S., Clement, G., Zarattini, M., Dellero, Y., Le Hir, R. et al. (2022) DspA/E-triggered non-host resistance against *E. amylovora* depends on the *Arabidopsis GLYCOLATE OXIDASE 2* gene. *International Journal of Molecular Sciences*, 23, 4224.

Li, J., Deng, F., Wang, H., Qiang, X., Meng, Y. & Shan, W. (2022) The Raf-like kinase Raf36 negatively regulates plant resistance against the oomycete pathogen *Phytophthora parasitica* by targeting MKK2. *Molecular Plant Pathology*, 23, 530–542.

Li, L., Li, M., Yu, L., Zhou, Z., Liang, X., Liu, Z. et al. (2014) The FLS2-associated kinase BIK1 directly phosphorylates the NADPH oxidase RbohD to control plant immunity. *Cell Host & Microbe*, 15, 329–338.

Li, Q., Ai, G., Shen, D., Zou, F., Wang, J., Bai, T. et al. (2019) A *Phytophthora capsici* effector targets ACD11 binding partners that regulate ROS-mediated defense response in *Arabidopsis*. *Molecular Plant*, 12, 565–581.

Li, W., Liu, Z., Huang, Y., Zheng, J., Yang, Y., Cao, Y. et al. (2024) *Phytophthora infestans* RXLR effector Pi23014 targets host RNA-binding protein NbRBP3a to suppress plant immunity. *Molecular Plant Pathology*, 25, e13416.

Li, W., Zhao, D., Dong, J., Kong, X., Zhang, Q., Li, T. et al. (2020) *AtRTP5* negatively regulates plant resistance to *Phytophthora* pathogens by modulating the biosynthesis of endogenous jasmonic acid and salicylic acid. *Molecular Plant Pathology*, 21, 95–108.

Li, X. (2017) *Regulation and function of association-dissociation of glycolate oxidase with catalase in rice* [PhD thesis]. Guangzhou: South China Agricultural University.

Li, X., Liao, M., Huang, J., Xu, Z., Lin, Z., Ye, N. et al. (2021) Glycolate oxidase-dependent H_2O_2 production regulates IAA biosynthesis in rice. *BMC Plant Biology*, 21, 326.

Lin, Y., Hu, Q., Zhou, J., Yin, W., Yao, D., Shao, Y. et al. (2021) *Phytophthora sojae* effector Avr1d functions as an E2 competitor and inhibits ubiquitination activity of GmPUB13 to facilitate infection. *Proceedings of the National Academy of Sciences of the United States of America*, 118, e2018312118.

Lindqvist, Y. & Branden, C. (1985) Structure of glycolate oxidase from spinach. *Proceedings of the National Academy of Sciences of the United States of America*, 264, 3624–3628.

Linhoff, M.W., Garg, S.K. & Mandel, G. (2015) A high-resolution imaging approach to investigate chromatin architecture in complex tissues. *Cell*, 163, 246–255.

Liu, R., Chen, T., Yin, X., Xiang, G., Peng, J., Fu, Q. et al. (2021) A *Plasmopara viticola* RXLR effector targets a chloroplast protein PsbP to inhibit ROS production in grapevine. *The Plant Journal*, 106, 1557–1570.

Liu, Y., Wu, W. & Chen, Z. (2018) Structures of glycolate oxidase from *Nicotiana benthamiana* reveal a conserved pH sensor affecting the binding of FMN. *Biochemical and Biophysical Research Communications*, 503, 3050–3056.

Lu, W., Deng, F., Jia, J., Chen, X., Li, J., Wen, Q. et al. (2020) The *Arabidopsis thaliana* gene *AtERF019* negatively regulates plant resistance to *Phytophthora parasitica* by suppressing PAMP-triggered immunity. *Molecular Plant Pathology*, 21, 1179–1193.

Mariyam, S., Sadiq, S., Ali, Q., Haider, M.S., Habib, U. et al. (2023) Identification and characterization of *Glycolate oxidase* gene family in garden lettuce (*Lactuca sativa* cv. 'Salinas') and its response under various biotic, abiotic, and developmental stresses. *Scientific Reports*, 13, 19686.

Meng, Y., Zhang, Q., Zhang, M., Gu, B., Huang, G., Wang, Q. et al. (2015) The protein disulfide isomerase 1 of *Phytophthora parasitica* (PpPDI1) is associated with the haustoria-like structures and contributes to plant infection. *Frontiers in Plant Science*, 6, 632.

Noctor, G., Veljovic-Jovanovic, S., Driscoll, S., Novitskaya, L. & Foyer, C.H. (2002) Drought and oxidative load in the leaves of C3 plants: a predominant role for photorespiration? *Annals of Botany*, 89, 841–850.

Olsen, L.J. & Harada, J.J. (1995) Peroxisomes and their assembly in higher plants. *Annual Review of Plant Physiology and Plant Molecular Biology*, 46, 123–146.

Petre, B., Contreras, M.P., Bozkurt, T.O., Schattat, M.H., Sklenar, J., Schornack, S. et al. (2021) Host-interactor screens of *Phytophthora infestans* RXLR proteins reveal vesicle trafficking as a major effector-targeted process. *The Plant Cell*, 33, 1447–1471.

Reumann, S., Buchwald, D. & Lingner, T. (2012) *PredPlantPTS1*: a web server for the prediction of plant peroxisomal proteins. *Frontiers in Plant Science*, 3, 194.

Reumann, S., Ma, C., Lemke, S. & Babujee, L. (2004) AraPerox. A database of putative *Arabidopsis* proteins from plant peroxisomes. *Plant Physiology*, 136, 2587–2608.

Rojas, C.M. & Mysore, K.S. (2012) Glycolate oxidase is an alternative source for H_2O_2 production during plant defense responses and functions independently from NADPH oxidase. *Plant Signaling & Behavior*, 7, 752–755.

Schmidt, A., Machtel, R., Ammon, A., Engelsdorf, T., Schmitz, J., Maurino, V.G. et al. (2020) Reactive oxygen species dosage in *Arabidopsis* chloroplasts can improve resistance towards *Colletotrichum higginsianum* by the induction of WRKY33. *New Phytologist*, 226, 189–204.

Schmitz, J., Hudig, M., Meier, D., Linka, N. & Maurino, V.G. (2020) The genome of *Ricinus communis* encodes a single glycolate oxidase with different functions in photosynthetic and heterotrophic organs. *Planta*, 252, 100.

Siddiqui, M.H., Alamri, S., Nasir Khan, M., Corpas, F.J., Al-Amri, A.A., Alsubaie, Q.D. et al. (2020) Melatonin and calcium function synergistically to promote the resilience through ROS metabolism under arsenic-induced stress. *Journal of Hazardous Materials*, 398, 122882.

Sun, Y., Li, P., Deng, M., Shen, D., Dai, G., Yao, N. et al. (2017) The *Ralstonia solanacearum* effector RipAK suppresses plant hypersensitive response by inhibiting the activity of host catalases. *Cellular Microbiology*, 19, e12736.

Wang, S., McLellan, H., Bukharova, T., He, Q., Murphy, F., Shi, J. et al. (2019) *Phytophthora infestans* RXLR effectors act in concert at diverse subcellular locations to enhance host colonization. *Journal of Experimental Botany*, 70, 343–356.

Wang, Z., Li, T., Zhang, X., Feng, J., Liu, Z., Shan, W. et al. (2023) A *Phytophthora infestans* RXLR effector targets a potato ubiquitin-like domain-containing protein to inhibit the proteasome activity and hamper plant immunity. *New Phytologist*, 238, 781–797.

Waypa, G.B., Marks, J.D., Guzy, R., Mungai, P.T., Schriewer, J., Dokic, D. et al. (2010) Hypoxia triggers subcellular compartmental redox signaling in vascular smooth muscle cells. *Circulation Research*, 106, 526–535.

Xu, H.W., Ji, X.M., He, Z.H., Shi, W.P., Zhu, G.H., Niu, J.K. et al. (2006) Oxalate accumulation and regulation is independent of glycolate oxidase in rice leaves. *Journal of Experimental Botany*, 57, 1899–1908.

Xu, Y.P., Yang, J. & Cai, X.Z. (2018) Glycolate oxidase gene family in *Nicotiana benthamiana*: genome-wide identification and functional analyses in disease resistance. *Scientific Reports*, 8, 8615.

Xue, D., Liu, H., Wang, D., Gao, Y. & Jia, Z. (2021) Comparative transcriptome analysis of *R3a* and *Avr3a*-mediated defense responses in transgenic tomato. *PeerJ*, 9, e11965.

Yang, M., Li, Z., Zhang, K., Zhang, X., Zhang, Y., Wang, X. et al. (2018) *Barley stripe mosaic virus* γb interacts with glycolate oxidase and inhibits peroxisomal ROS production to facilitate virus infection. *Molecular Plant*, 11, 338–341.

Yang, Y., Zhao, Y., Zhang, Y., Niu, L., Li, W., Lu, W. et al. (2022) A mitochondrial RNA processing protein mediates plant immunity to a broad spectrum of pathogens by modulating the mitochondrial oxidative burst. *The Plant Cell*, 34, 2343–2363.

Yin, J., Gu, B., Huang, G., Tian, Y., Quan, J., Lindqvist-Kreuze, H. et al. (2017) Conserved RXLR effector genes of *Phytophthora infestans* expressed at the early stage of potato infection are suppressive to host defense. *Frontiers in Plant Science*, 8, 2155.

Yin, X., Fu, Q., Shang, B., Wang, Y., Liu, R., Chen, T. et al. (2022) An RxLR effector from *Plasmopara viticola* suppresses plant immunity in grapevine by targeting and stabilizing VpBPA1. *The Plant Journal*, 112, 104–114.

Zhang, H., Li, F., Li, Z., Cheng, J., Chen, X., Wang, Q. et al. (2021) Potato StMPK7 is a downstream component of StMKK1 and promotes resistance to the oomycete pathogen *Phytophthora infestans*. *Molecular Plant Pathology*, 22, 644–657.

Zhang, M., Chiang, Y.H., Toruno, T.Y., Lee, D., Ma, M., Liang, X. et al. (2018) The MAP4 kinase SIK1 ensures robust extracellular ROS burst and antibacterial immunity in plants. *Cell Host & Microbe*, 24, 379–391.

Zhang, Q. (2019) *Functional analysis of the effector proteins Pp18 and PpCys44/45 secreted by* Phytophthora parasitica [PhD thesis]. Yangling: The Northwest A&F University.

Zhang, Q., Li, W., Yang, J., Xu, J., Meng, Y. & Shan, W. (2020) Two *Phytophthora parasitica* cysteine protease genes, *PpCys44* and *PpCys45*, trigger cell death in various *Nicotiana* spp. and act as virulence factors. *Molecular Plant Pathology*, 21, 541–554.

Zhang, T. (2020) En garde: CRK2 preassociates with RBOHD and regulates ROS production. *The Plant Cell*, 32, 801–802.

Zhang, Y. & Li, X. (2019) Salicylic acid: biosynthesis, perception, and contributions to plant immunity. *Current Opinion in Plant Biology*, 50, 29–36.

Zhang, Z., Xu, Y., Xie, Z., Li, X., He, Z.H. & Peng, X.X. (2016) Association-dissociation of glycolate oxidase with catalase in rice: a potential switch to modulate intracellular H_2O_2 levels. *Molecular Plant*, 9, 737–748.

Zhong, Z., Wang, Y., Wang, M., Yang, F., Thomas, Q.A., Xue, Y. et al. (2022) Histone chaperone ASF1 mediates H3.3-H4 deposition in *Arabidopsis*. *Nature Communications*, 13, 6970.

SUPPORTING INFORMATION

Additional supporting information can be found online in the Supporting Information section at the end of this article.

How to cite this article: Zhang, P., Li, J., Gou, X., Zhu, L., Yang, Y., Li, Y. et al. (2024) The *Phytophthora infestans* effector Pi05910 suppresses and destabilizes host glycolate oxidase StGOX4 to promote plant susceptibility. *Molecular Plant Pathology*, 25, e70021. Available from: https://doi.org/10.1111/mpp.70021